2018 Annual American Control Conference (ACC)
June 27–29, 2018. Wisconsin Center, Milwaukee, USA

Modeling of Pneumatic Artificial Muscle with Kinetic Friction and Sliding Mode Control

Jonathon E. Slightam* and Mark L. Nagurka*

Abstract—**A nonlinear lumped-parameter state-space model of a pneumatic artificial muscle that accounts for kinetic friction is developed. Model simulations are reported for square-wave command signals at different frequencies. Comparisons to experimental results demonstrate the fidelity of the model. A new sliding mode control tuning parameter is introduced that increases the gradient of the error dynamic poles of the sliding surface with respect to lower order errors. With this method input-output feedback linearization and model observation are not needed. A third-order integral sliding mode control law exhibits steady-state errors of $\pm$ 15 μm or less with a maximum error of 0.29 mm or less when tracking a 7th-order square-wave position trajectory with an amplitude of 5.40 mm. This simplified sliding mode control law shows advantages compared to a conventional approach.**

Index Terms—**Fluid-Power Control, Sliding Mode Control, Modeling, Pneumatic Artificial Muscles.**

I. Introduction

A pneumatic artificial muscle (PAM) is a flexible actuator constructed from a hyperelastic tube inside of a braided fiber sleeve with caps on both ends. One end allows a compressed gas (typically air) to flow in and out. When pressurized, the tube and braid assembly deforms radially and contracts longitudinally resulting in a force and displacement that is analogous to biological muscle [1].

PAMs are often deployed in antagonistic pairs and use computationally expensive model-based controllers to achieve high performance. As soft robots include more and more degrees of freedom, computational costs from model-based controllers can become a technical hurdle. The challenge addressed here is to design a model-based control system that has similar computational requirements of classical methods with the performance of model-based methods.

This paper presents a nonlinear lumped-parameter model of a PAM with a new expression for kinetic friction and a novel control approach. A background on PAM modeling and control approaches is first presented. Then detailed modeling of the actuator dynamics, pressure dynamics, and overall system dynamics of a PAM is developed. Subsequently, a novel design of a sliding mode position controller is presented. This is followed by a description of the experimental setup, results of the simulations and experiments, and a discussion with conclusions.

*Jonathon E. Slightam is a Ph.D. candidate in Marquette University's Department of Mechanical Engineering. Mark L. Nagurka is an associate professor in the Department of Mechanical Engineering and director of the Fluid Power and Mechatronics Research Laboratory.

II. Background

The first patent for a PAM, an *Apparatus for Generating an Over-or-Under Pressure in Gases or Liquids* in 1929, was followed by patents by Morin, Woods, and Gaylord, as well as by McKibben, who used a PAM in an orthotic device [2]. PAMs are sometimes referred to as McKibben actuators, despite the foundational work by Gaylord and others [3], [4]. Although in use for almost a century, their theoretical behavior is still under study.

A. Modeling of PAMs

Using a discrete transfer function and experimentally determined parameters, Caldwell *et al.* developed a dynamic model and discrete closed-loop control systems for PAMs [5]. Paynter and Nagurka modeled PAMs for active leveling, tuning, and damping of vehicle suspensions and motor mounts and illustrated the position dependent nature of their force output [6].

Driver and Shen modeled a sleeved PAM using Chou and Hannaford's force model and a rotational spring-mass-damper model [7], [8]. Driver and Shen also incorporated pressure dynamics with idealized valve dynamics, with the latter being popularized by Richer and Hurmuzlu, with the command input being the valve position or aperture area of the valve [9].

Kang *et al.* modeled an antagonistic pair of PAMs for a rotational joint and arrived at a similar expression as Driver and Shen and Tang without using a spring term [10], [11]. Kang's friction model came from the form of Tondu's, whose dynamic model was presented as an empirical three parameter model for the dynamic dry friction due to the contact surface of the shell against itself (the braid against the rubber tube) [12].

Hošovský and Havran presented an empirical model with nonlinear terms for the force, damper, and spring based on a modified Hill's model with a variable damper, which was later used and refined by Tóthová and Pitel' *et al* [13]–[17].

A multivariate damping term was introduced to describe the damping force as $F_D = \mu P\dot{\zeta}$ or $F_D = \mu P\dot{x}$, where $\dot{\zeta}$ is the rate of the contraction ratio, $\dot{x}$ is the rate of displacement, and μ is the area normalized geometric coefficient to model the viscous friction between the braid and bladder [18], [19]. In [18], this damping force is a single damping term, whereas Slightam and Nagurka modeled the damping force as $F_D = \mu P\dot{x} + c\dot{x}$, where the linear damping term reflects of the braid on braid friction and viscous friction from bearings and bushings [19], [20]. This paper expands this concept using an analytical approach and develops a dynamic PAM model.

B. Control

Model-based nonlinear control techniques have proven to be practical and superior in many cases to linear control theory for pneumatic applications. Sliding mode control (SMC) approaches for the motion control of pneumatic flexible actuators have been used due to their ability to converge the error dynamics to zero over a given trajectory [21]. Comber *et al.* applied a SMC on a pneumatic five degree of freedom steerable needle robot that exhibited needle tip errors of 0.78 mm or less, smaller than the voxel size of most MRI machines [22]. De Volder *et al.* achieved positioning accuracy of $\pm$30 μm using PI-SMC [23]. Slightam *et al.* presented a PI-SMC that attained steady-state accuracy of 50 μm [19]. Liu *et al.* proposed two types of SMC for PAMs based on an empirical model, and compared the SMCs to a PID control law showing approximately half the error for sinusoidal tracking [24].

III. Modeling

This paper derives a lumped-parameter model of a PAM, where the multivariate kinetic friction term previously introduced by Slightam and Nagurka is expanded [19]. Model simulations are compared to experimental results motivating a new SMC design.

A. Actuator Dynamics

The PAM consists of a rubber tube encompassed by a helical fiber braid with end caps, as shown in Fig. 1 (left). The length L of the PAM is

$$L = L_0 - x \tag{1}$$

where L_0 is the initial length and x is the displacement of the free end of the PAM. The length L is also related to the helical fiber length, b, of the braid that wraps around the rubber tube and angle of the fiber relative primary axis by $L = b\cos\theta$. The model of the PAM is shown in Fig. 1 (right). The force from the PAM as a result of pressurization is determined using the principle of virtual work [3], [7].

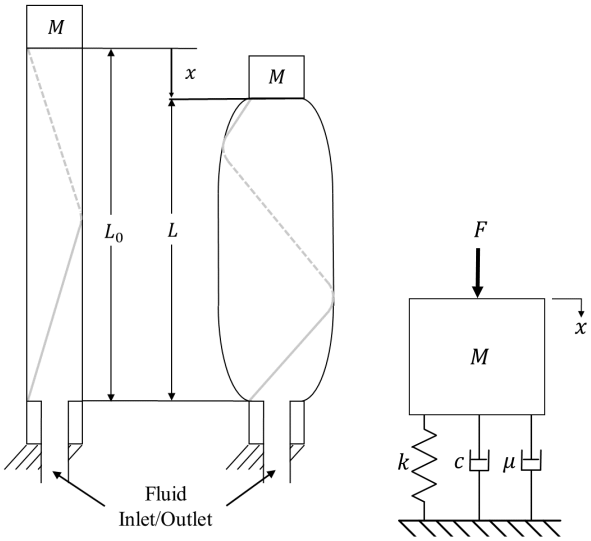

Fig. 1: Pneumatic Artificial Muscle Diagram and Model [19].

The volume of the PAM is defined by

$$V = \frac{L(b^2 - L^2)}{4\pi n^2} \tag{2}$$

where n is the number of turns the fiber braid wraps around the rubber tube. Using the principle of virtual work, $F = -PdV/dL$, from Eqn. 2, the force produced by the actuator is

$$F = \frac{P(3L^2 - b^2)}{4\pi n^2}. \tag{3}$$

This force represents the input to the equation of motion from Newton's second law,

$$M\ddot{x} + F_f(x, \dot{x}, P) + kx = \frac{P(3L^2 - b^2)}{4\pi n^2}, \tag{4}$$

where k is the stiffness of the actuator material which is assumed to linear at the PAMs given operating pressure, P is the internal pressure, $F_f(x, \dot{x}, P)$ is the kinetic friction model that describes the friction between the tube and fiber braid in addition to the internal damping of the tube, and M is the mass of the non-fixed end of the PAM. The friction model is

$$F_f = \begin{cases} c\dot{x} + \mu_k NPA_b(b\dot{\theta}\cos\theta + \dot{x}) & \dot{x} > 0 \\ c\dot{x} & \dot{x} < 0 \end{cases} \tag{5}$$

where μ_k is the coefficient of kinetic friction between the rubber tube and the braid, N is the number of braids in the braid assembly, and A_b is the area of a single braid in contact with the tube, which can be determined using a Hertzian contact model and measurements of the braid strand thickness and the length of the braid b. The other friction force term, $c\dot{x}$, represents the internal damping of the material and braid-to-braid Coulomb friction.

In state-space form, Eqn. 5 can be expressed as

$$\begin{pmatrix} \dot{x}_1 \\ \dot{x}_2 \end{pmatrix} = \begin{pmatrix} x_2 \\ \frac{P(3(L_0-x_1)^2-b^2)}{4\pi M n^2} - \frac{F_f(x_1,x_2,P)}{M} - \frac{kx_1}{M} \end{pmatrix} \quad (6)$$

The actuator model parameters are listed in Table I.

TABLE I: ACTUATOR PARAMETERS.

Parameter	Value	Parameter	Value
M	0.05 kg	L_0	200 mm
c	0.57 N-s/mm	b	232 mm
n	1.94	k	9.68 N/mm
μ_k	55.3	D	19.1 mm
N	100	A_b	0.233 mm^2

B. Pressure Dynamics

The pressure dynamics for the PAM are modeled for the actuator control volume and a proportional flow control valve. The pressure rate of change of the control volume is the time derivative of the ideal gas law,

$$\dot{P} = \frac{RT}{V}\dot{m} - \frac{P}{V}\dot{V}, \quad (7)$$

where R is the universal gas constant for air, T is the absolute temperature of the air, V is the volume of the actuator, $\dot{V}$ is the rate of change of volume, and $\dot{m}$ is the mass flow rate. The pressure dynamics model is explained in more detail in [22], [25], [26] and [9].

The mass flow rate is modeled as isentropic flow through a plate with a small hole (aperture). The mass flow rate is described by $\dot{m} = A_v\Psi$, where the aperture area A_v is assumed to be linearly proportional to the valve command voltage ($A_v = K_{A_v}u$) and the area normalized flow rate Ψ is a piecewise function governed by choked and unchoked flow regimes that is based on the quotient of the downstream and upstream pressures, $\Psi(P_u, P_d) = \Psi_c\frac{P_d}{P_u} \leq C_r$ for choked flow and $\Psi(P_u, P_d) = \Psi_{uc}\frac{P_d}{P_u} > C_r$ for unchoked flow regimes, described and validated in [9] and applied to PAMs in [8], [27], and [19].

In state-space form, the PAM pressure dynamics are

$$\dot{P} = \dot{x_3} = \frac{RTK_{Av}\Psi}{V(x_1)}u - \frac{x_3\dot{V}(x_1,x_2)}{V(x_1)} \quad (8)$$

with u being the command voltage ($\pm$ 5 V) and K_{Av} is the aperture area gain. Parameter values are listed in Table II.

TABLE II: PNEUMATIC SYSTEM PARAMETERS.

Parameter	Value	Parameter	Value
P_{tank}	441.3 kPa	A_v	$\pm$ 5.161 mm^2
P_{atm}	101.3 kPa	T	273.0 K
R	287.1 J kg^{-1} K^{-1}	K_{A_v}	1.03 mm^{2}V^{-1}

C. System Dynamics

The system dynamics for the servovalve controlled PAM include Eqn. 6 and 8. In state-space form,

$$\dot{x} = \begin{pmatrix} x_2 \\ \frac{x_3(3(L_0-x_1)^2-b^2)}{4\pi M n^2} - \frac{F_f(x_1,x_2,x_3)}{M} - \frac{kx_1}{M} \\ \frac{RTK_{Av}\Psi}{V(x_1)}u - \frac{x_3\dot{V}(x_1,x_2)}{V(x_1)} \end{pmatrix}. \quad (9)$$

IV. SLIDING MODE POSITION CONTROL

Traditional SMC approaches for PAMs use an integral sliding surface $s = \left(\frac{d}{dt} + \lambda\right)^m \int e$, where m is the order of the differential equation of the system to be controlled [21], [25], [27]. This results in a 3rd-order sliding surface for a PAM tracking control problem. It is proposed that the constant λ be raised to the power q to increase the gradient of the error dynamic poles from absement (integral of position) to position and higher order terms [28] [19]. Then the sliding surface is

$$s = \left(\frac{d}{dt} + \lambda^q\right)^m \int e \quad (10)$$

where q is a new tuning parameter. For a PAM, where $m = 3$, expanding Eqn. 10,

$$s = \ddot{e} + 3\lambda^q\dot{e} + 3\lambda^{2q}e + \lambda^{3q}\int e. \quad (11)$$

Differentiating Eqn. 11 with respect to time

$$\dot{s} = \dddot{e} + 3\lambda^q\ddot{e} + 3\lambda^{2q}\dot{e} + \lambda^{3q}e. \quad (12)$$

The equivalent control law can be expressed using Filippov's equivalent dynamics principle

$$u_{eq} = \frac{1}{\hat{g}}\left(\dddot{x}_D + \hat{f} - 3\lambda^q\ddot{e} - 3\lambda^{2q}\dot{e} - \lambda^{3q}e\right) \quad (13)$$

where $\hat{f}$ and $\hat{g}$ are model estimation parameters determined by solving for the control input in the third order model, similar to those presented in [27], [25]. With a Lyapunov like function, $\frac{1}{2}\frac{d}{dt}s^2 \leq -\eta \mid s \mid$, the robust control law is determined to be

$$u_{rb} = \eta \mid s \mid sgn(s) \quad (14)$$

to keep the sliding surface s at zero, where $sgn(s) = +1$ if $s > 0$ and $sgn(s) = -1$ if $s < 0$. To minimize chatter from the high speed switching, a saturation function is introduced to act as a first-order filter, with the saturation of s/ϕ being at ± 1, where ϕ is a constant that decreases the rate of switching.

$$u_{rb} = \eta \mid s \mid sat\left(\frac{s}{\phi}\right) \quad (15)$$

Combining the equivalent and robust control laws and introducing a proportional gain, K_p, results in the 3rd-order integral sliding surface SMC law,

$$u_{SMC} = \frac{K_p}{\hat{g}}\left(\dddot{x}_D + \hat{f} - 3\lambda\ddot{e}^q - 3\lambda^{2q}\dot{e} - \lambda^{3q}e - u_{rb}\right) \quad (16)$$

with the tuning parameter q. With the parameter q, the control law is assumed sufficiently robust such that observation and input-output feedback linearization are not needed. Eliminating $\hat{f}$ and $\hat{g}$, the SMC becomes

$$u_{qSMC} = K_p\left(\ddot{x}_D - 3\lambda^q\ddot{e} - 3\lambda^{2q}\dot{e} - \lambda^{3q}e - u_{rb}\right) \quad (17)$$

For benchmark comparison, a traditional SMC using observation, where $q = 1$, is

$$u_{SMC} = \frac{K_p}{\hat{g}}\left(\ddot{x}_D + \hat{f} - 3\lambda\ddot{e} - 3\lambda^2\dot{e} - \lambda^3 e - u_{rb}\right) \quad (18)$$

The tuning parameters determined empirically for both control laws are listed in Table III. Both SMCs were tuned by first adjusting the parameter λ, followed by incrementally increasing η to achieve the desired tracking while simultaneously increasing ϕ to eliminate chatter. The new controller was tuned by simultaneously adjusting λ and q. Two 3rd-order low-pass filters were used to filter the measured encoder signal and numerical differentiation noise for error dynamic and observer derivatives; these are denoted as LPF_1 and LPF_2, respectively.

TABLE III: SMC PARAMETERS.

SMC Parameter	Eqn. (17) Value	*qSMC* Parameter	Eqn. (16) Value
LPF_1	300 Hz	LPF_1	300 Hz
LPF_2	0.5 Hz	LPF_2	0.5 Hz
K_p	0.00025	K_p	0.0002
λ	225 Hz	λ	10 Hz
η	25.4 mm/s^3	η	10.2 mm/s^3
ϕ	2.54 mm/s^2	ϕ	0.51 mm/s^2
q	1	q	1.75

V. Experimental Setup

The PAM is controlled and tested via Simulink Desktop Real-time operating at 1 kHz with a desktop computer using a National Instruments PCI-6221 data acquisition card (DAQ). The PAM test stand is shown in the upper image of Fig. 2 with the PAM shown in the lower image of Fig. 2.

An Enfield Technologies LS-V05s proportional pneumatic control valve is used that has a bandwidth of 109 Hz. A voltage command signal is sent from the DAQ to an Enfield Technologies D1 proportional linear motor valve driver. The proportional flow control valve controls the mass flow rate from the pressure source at the manifold to the PAM or from the PAM exhausted to atmosphere. Between the valve and the PAM, a NPX MPX5700GP pressure sensor is used to record the pressure dynamics. The PAM's guide shaft is connected to a US Digital EM2 optical quadrature encoder with 2000 counts per 25.4 mm (1 inch), giving a resolution of 3.2 μm.

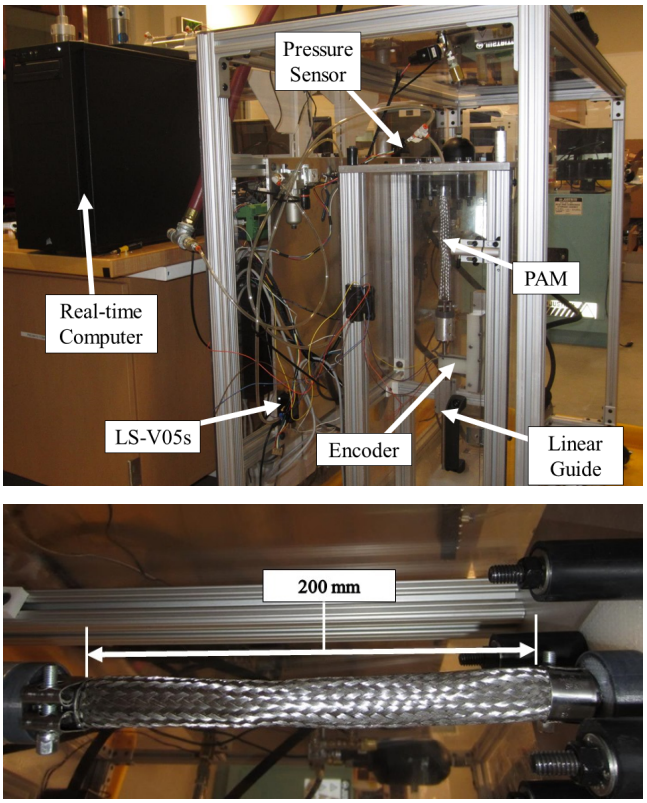

Fig. 2: Experimental Setup For PAM Testing and PAM tested.

VI. Simulation and Experimental Results

A. Model Simulation vs. Physical System

For model validation, a square wave voltage command signal was applied to the valve controller and the response of the PAM was measured. Experiments were conducted at frequencies of 0.25, 0.5, 1, and 2 Hz and at amplitudes of the maximum voltage (5 V) with 5 V offset (0 to 10 V command signal). The open-loop responses of the square-wave command signal at 0.25, 0.5, 1, and 2 Hz are shown in Fig. 3, which demonstrates accurate model prediction for the position of the PAM at the four command signals.

B. Controller Tracking Experiments

Two different tracking experiments were conducted: in experiment 1, a square-like seventh-order polynomial trajectory with an amplitude of 5.4 mm and an offset of 11.8 mm, with 0.2 Hz transitions between set points and a 0.1 Hz resting period, is tracked; in experiment 2, the same trajectory with no steady-state period is tracked. Fig. 4 and 5 show the results of the tracking experiments 1 and 2, respectively.

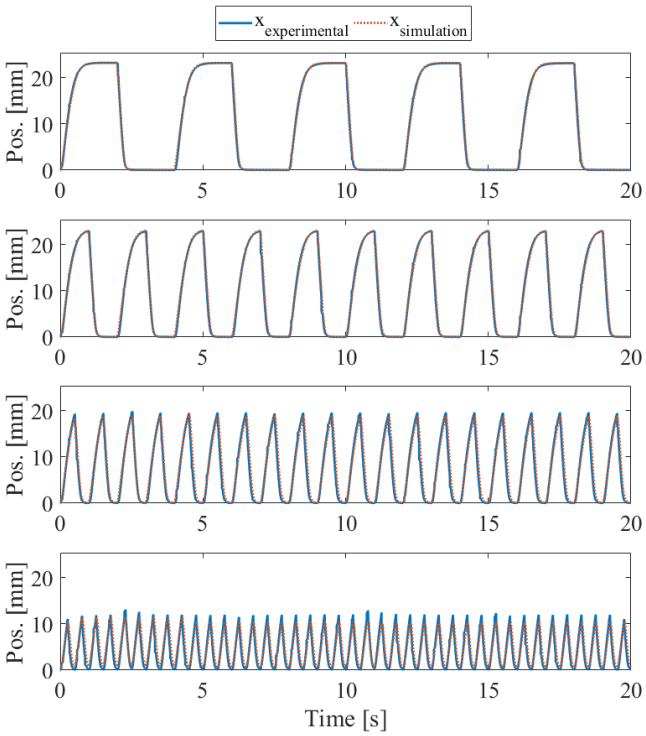

Fig. 3: 0.25, 0.5, 1, AND 2 HZ SQUARE WAVE RESPONSES OF ACTUAL AND MODEL.

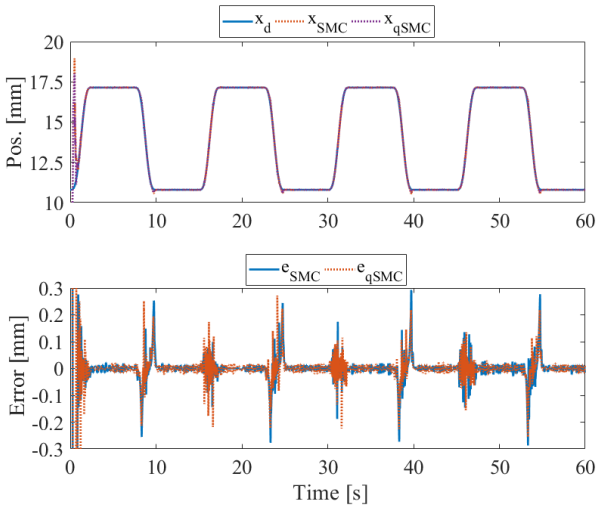

Fig. 4: TRACKING EXPERIMENT 1.

The 7th-order trajectory is determined by methods presented in Niku and is needed to provide a continuous-time trajectory for higher order differential terms in the control law [29]. The maximum tracking, steady-state (s.s.), and root-mean-square (RMS) errors for both controllers and experiments are listed in Table IV.

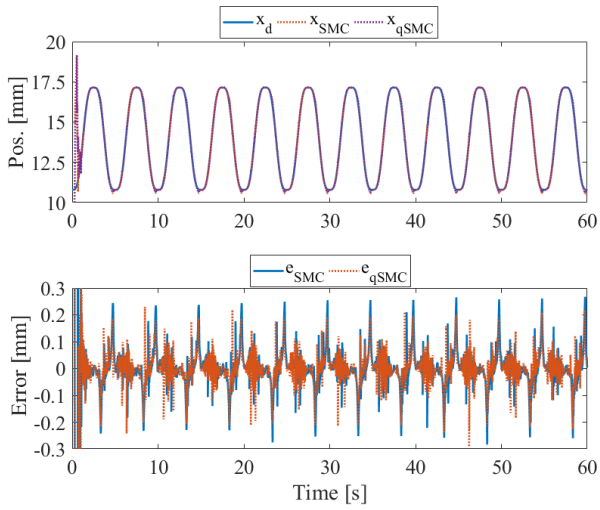

Fig. 5: TRACKING EXPERIMENT 2.

TABLE IV: CONTROLLER PERFORMANCE.

Index	Experiment	SMC	qSMC
max($\|e\|$)	1	292 µm	272 µm
s.s. e	1	$\pm$ 15 µm	$\pm$ 15 µm
RMS(e)	1	43.2 µm	35.6 µm
max($\|e\|$)	2	284 µm	291 µm
RMS(e)	2	43.2 µm	55.3 µm

The controllers in both tracking experiments exhibit tracking errors of 0.3 mm or less. For the tracking experiment with a 10 s resting period the steady-state accuracy of the controller was 15 µm for both controllers.

VII. DISCUSSION

Comparing the results of the model and the actual system shows that the PAM model accurately predicts the dynamic behavior. There is slight degradation in the accuracy of the model at higher frequencies likely due to discrepancies in valve and pressure dynamics.

The SMC law with the exponential modifier shows that accurate sub-millimeter tracking is possible without observers and input-output feedback linearization. There is a small difference in the controller performance between methods, as shown in Table IV. This suggests that the simplified SMC is sufficiently robust that observation and input-output feedback linearization are unwarranted. This promises to be particularly useful in soft robotic applications where there are many degrees of freedom and computationally expensive controllers may be problematic.

VIII. CONCLUSIONS

A dynamic lumped-parameter model of a PAM that includes kinetic friction is presented. A comparison of model simulation and experimental results from a

square wave command to the valve at 0.25, 0.5, 1, and 2 Hz shows high fidelity.

Based on the model, a sliding mode control law is derived using a 3rd-order integral sliding surface. A tuning parameter q is added that is the exponent of λ in the integral sliding surface function. It allows for the error dynamic poles to be manipulated so model observation and input-output feedback linearization are not needed. This simplified SMC method is compared to a traditional approach with no discernable difference in tracking performance. With the simplified SMC, measurement of the position of the PAM provides sufficient information to achieve sub-millimeter tracking. This approach requires tuning of five parameters (λ, K_p, η, ϕ, and q), making implementation nearly as simple as PID control (that requires tuning of K_P, K_I, K_D, and n) with exclusion of model estimation.

REFERENCES

[1] B. Hannaford and J. Winters, *Actuator Properties and Movement Control: Biological and Technical Models*. Springer-Verlag, New York, 1990, pp. 101–120.

[2] D. S. D. Lavaud, "Apparatus for Generating an Over-or-Under Pressure in Gases or Liquids," *German Patent DE503775C*, 1929.

[3] R. Gaylord, "Fluid Actuated Motor System and Stroking Device," *US Patent 2844126*, 1957.

[4] L. Barber and V. Nickel, "Carbon dioxide-powered arm and hand devices," *The American Journal of Occupational Therapy*, vol. 23, no. 3, pp. 215–225, 1969.

[5] D. Caldwell, A. Razak, and M. Goodwin, "Braided Pneumatic Artificial Muscle Actuators," *IFAC Conference on Intelligent Autonomous Vehicles*, pp. 507–512, 1993.

[6] H. Paynter and M. Nagurka, "Hybrid Tension-Compression Pneumatic Actuators for Active Leveling, Tuning, and Damping of Vehicle Suspensions and Engine Mounts," *Proceedings of the 1997 IEEE Conference on Control Applications*, pp. 630–632, Oct. 1997.

[7] C.-P. Chou and B. Hannaford, "Measurement and Modeling of McKibben Pneumatic Artifical Muscles," *IEEE Transactions on Robotics and Automation*, vol. 12, no. 1, 1996.

[8] T. A. Driver and X. Shen, "Design and Control of a Sleeve Muscle-Actuated Robot Elbow," *ASME Journal of Dynamic Systems, Measurement, and Control*, vol. 136, no. 1, 2014.

[9] E. Richer and Y. Hurmuzlu, "A High Performance Pneumatic Force Actuator System: Part 1 - Nonlinear Mathematical Model," *ASME Journal of Dynamic Systems, Measurement, and Control*, vol. 122, no. 3, pp. 416–425, 2000.

[10] B. Kang, C. Kothera, B. Woods, and N. Wereley, "Dynamic Modeling of McKibben Pneumatic Artificial Muscles for Antagonistic Actuation," *2009 International Conference on Robotics and Automation*, pp. 182–187, May 12-17, 2009.

[11] T. Tang, S. Chong, M. Tan, C. Chan, and K. Sato, "Characterization of Pneumatic Artificial Muscle System in an Opposing Pair Configuration," *Journal of Telecommunications, Electronic and Computer Engineering*, vol. 8, no. 2, pp. 73–77, 2016.

[12] B. Tondu and P. Lopez, "Modeling and Control of McKibben Artificial Muscle Robot Actuators," *IEEE Control Systems Magazine*, vol. 20, no. 2, pp. 15–38, 2000.

[13] T. Kerscher, J. Albiez, J. Zollner, and R. Dillmann, "Evaluation of the Dynamic Model of Fluidic Muscles using Quick-Release," *International Conference on Biomedical Robotics and Biomechatronics*, pp. 637–642, 20-22 Feb. 2006.

[14] A. Hošovský and M. Havran, "Dynamic Modeling of One Degree of Freedom Pneumatic Muscle-Based Actuator for Industrial Applications," *Technical Gazette*, vol. 19, no. 3, 2012.

[15] M. Tóthová and J. Piteĺ, "Dynamic Model of Pneumatic Actuator Based on Advanced Geometric Muscle Model," *IEEE 9th International Conference on Computational Cybernetics*, pp. 82–87, 8-10 July 2013.

[16] M. Tóthová and J. Piteĺ, "Simulation of Actuator Dynamics Based on Geometric Model of Pneumatic Artificial Muscle," *IEEE 11th International Symposium on Intelligent Systems and Informatics*, pp. 233–237, 26-28 Sept. 2013.

[17] J. Piteĺ and M. Tóthová, "Dynamic Modeling of PAM based Actuator Using Modified Hill's Muscle Model," *IEEE Carpathian Control Conference*, pp. 307–310, 26-29 May 2013.

[18] A. Hošovský and M. Havran, "Dynamic Characterization and Simulation of Two-Link Soft Robot Arm with Pneumatic Muscles," *Mechanism and Machine Theory*, vol. 103, pp. 98–116, 2016.

[19] J. E. Slightam and M. L. Nagurka, "Robust Control Law of Pneumatic Artificial Muscles," *ASME/Bath Symposium on Fluid Power and Motion Control*, 16-19 Oct. 2017.

[20] S. Davis and D. G. Caldwell, "Braid Effects on Contractile Range and Friction Modeling in Pneumatic Artificial Muscles," *International Journal of Robotics*, vol. 25, no. 4, pp. 359–369, 2006.

[21] J. Slotine and W. Li, *Applied Nonlinear Control*. Prentice Hall, 1991.

[22] D. Comber, E. Barth, and R. Webster III, "Design and Control of an MR-Compatible Precision Pneuamtic Active Cannula Robot," *ASME J Medical Devices*, vol. 8, no. 1, 2014.

[23] M. D. Volder, J. Coosemans, R. Puers, and D. Reynaerts, "Characterization and Control of a Pneumatic Microactuator with Integrated Inductive Position Sensor," *Journal of Sensors and Actuators*, vol. 141, no. 1, pp. 192–200, 2008.

[24] H. Liu, Y. Zhao, F. Jiang, and X. Yao, "Pneumatic Muscle Actuator Position Control Based on Sliding Mode Control Algorithms," *Proceedings of the 2015 IEEE International Conference on Information and Automation*, pp. 1115–1120, Aug. 8-10 2015.

[25] D. B. Comber, J. E. Slightam, V. R. Gervasi, Webster III, R. J., and E. J. Barth, "Design and Precision Control of an MR-Compatible Flexible Fluidic Actuator," *Proc. ASME/Bath Symposium on Fluid Power and Motion Control*, Oct. 6-9 2013.

[26] Y. Zhu and E. J. Barth, "Accurate Sub-Millimeter Servo-Pneumatic Tracking Using Model Reference Adaptive Control (MRAC)," *International Journal of Fluid Power*, vol. 11, no. 2, pp. 49–57, 2010.

[27] J. E. Slightam and M. L. Nagurka, "PID Sliding Mode Control of Prolate Flexible Pneumatic Actuators," *Proceedings of the ASME 2016 International Dynamic Systems and Control Conference*, Oct. 12-14 2016.

[28] R. Janzen and S. Mann, "Actergy as a Reflex Performance Metric: Integral Kinematics Applications," *2014 IEEE Games Media Entertainment (GEM)*, Oct. 22-24 2014.

[29] S. Niku, *Introduction to Robotics - Analysis, Controls, Applications*, 2nd ed. Wiley, 2010.